Instability-Triggered Phase Transition to a Dusty-Plasma Condensate

Glenn Joyce,* Martin Lampe, and Gurudas Ganguli
Plasma Physics Division, Naval Research Laboratory, Washington, D.C. 20375-5346
(Received 2 October 2001; published 15 February 2002)

Highly charged dust grains in plasma discharges reside at the sheath edge, where the ions stream toward the electrode at speed $\sim c_s$. Above a critical pressure $P_{\rm crit}$, the grains lose their kinetic energy and reach a strongly coupled crystalline state, but for $P < P_{\rm crit}$ the grains acquire a large random kinetic energy and act like a fluid. We show that the dust heating in the fluid phase is due to an ion-dust two-stream instability, which is stabilized at $P > P_{\rm crit}$ by the combined effect of ion-molecule and grain-molecule collisions.

DOI: 10.1103/PhysRevLett.88.095006 PACS numbers: 52.27.Lw, 52.20.Dq, 52.25.–b

1. Introduction.—Micron-scale "dust grains" immersed in rf plasma discharges acquire a large negative charge $-Ze$ and settle into a dust cloud at the edge of the sheath over the lower electrode, where gravity is balanced by the repulsive force of the sheath electric field on the negative grains. For a typical case with electron temperature $T_e = 3$ eV and grain radius $a = 3.5$ μm, $Z \sim 15\,000$ and the screened interaction potential $\langle\phi\rangle$ between grains separated by 200 μm is $\sim$500 eV. At sufficiently high gas pressure P, the random kinetic energy of the grains is damped by gas friction, and the kinetic temperature T_d of the dust grains reaches a steady-state value <0.7 eV, the instrumental limit [1]. Since $T_d \lll \langle\phi\rangle$, the grains are strongly coupled and self-organize into a crystalline configuration. However, it is important that at the sheath edge, ions stream toward the electrode at a velocity $\mathbf{u} \sim c_s \equiv \sqrt{T_e/m_i}$, the ion sound speed. The ion flow creates an electrostatic wake downstream of each grain, and there are positively charged points in the wake structure behind each grain, which attract other grains. As a result, the grains line up directly behind each other along the streaming direction, but transverse to the streaming form a lattice which is usually hexagonal [1–6]. This type of crystal structure, known as simple hexagonal, never occurs in ordinary solids where the interactions between atoms are isotropic.

In lower pressure experiments, a very different behavior is seen. Despite the dissipation of grain kinetic energy to gas friction, the dust grains reach a steady-state kinetic temperature which is much larger than the temperature of any other component in the plasma. In fact, T_d is so large that the dust acts like a fluid [1,5]. If P is increased in real time, the dust cools down and freezes into a crystal. Conversely, an existing dust crystal melts as P is decreased. Schweigert *et al.* [6] and Melandso [7] have explained the melting in terms of an instability of the crystal phonons. However, these authors imply that the phonon instability disappears as the crystal structure melts. No explanation has been offered for the intense heating of dust in the fluid phase. Many possible mechanisms have been examined and have been shown to be inadequate [8].

In this Letter, we show analytically that an ion-grain two-stream instability is present at low pressure but is stabilized by the combined effects of ion-molecule and dust-molecule collisions at pressures above a critical $P_{\rm crit}$. Although streaming instabilities have been studied for over five decades, most recently in the context of dusty plasma [9], this Letter appears to be the first to show that the two-stream instability between two cold components can be stabilized by collisions. We then present homogeneous simulations that show strong dust heating for $P < P_{\rm crit}$, but very low T_d for $P > P_{\rm crit}$. Finally, we present simulations of the formation and evolution of bounded dust clouds, which cool and condense into a crystal with several crystal layers (at $P > P_{\rm crit}$), or heat and remain fluid (at $P < P_{\rm crit}$). The phase transition points seen in the dust cloud simulations agree with the stability limits from the theory and are also consistent with the experimental observations. We conclude that this instability is the cause of the observed dust heating, and the phase transition to a crystal state occurs when the instability is stabilized.

2. Analysis of the two-stream instability.—Consider a dusty plasma consisting of warm Boltzmann electrons with density n_e and Debye length $\lambda_{\rm De}$; ions with density n_i, plasma frequency ω_i, and streaming velocity $\mathbf{u}$; and dust in the fluid phase with density n_d and plasma frequency ω_d. Both the dust and the ions are subject to collisions with the neutral molecules, with momentum loss frequencies ν_d and ν_i, respectively. In situations of interest, the phase velocity of the most unstable waves is found to lie outside the thermal distribution of either the dust or the ions but well inside the electron distribution. Thus, both dust and ions can be regarded as cold, and the dispersion relation is

$$0 = 1 + \frac{1}{k^2\lambda_{\rm De}^2} - \frac{\omega_d^2}{\omega(\omega + i\nu_d)} - \frac{\omega_i^2}{(\omega - \mathbf{k}\cdot\mathbf{u})(\omega - \mathbf{k}\cdot\mathbf{u} + i\nu_i)}. \quad (1)$$

[It is assumed in (1) that the dust is a weakly coupled gaslike plasma species. This is appropriate for the specific cases discussed in this Letter, but is would be of

interest to extend the theory to include liquidlike correlations between dust grains.] Numerical solutions of Eq. (1) show that all modes are stable if *both* ν_d/ω_d and ν_i/ω_i are large enough, as shown in Fig. 1. For the particular case $\nu_d/\omega_d = \nu_i/\omega_i$ it can be shown analytically that the stability condition is

$$\frac{\nu_d}{\omega_d} = \frac{\nu_i}{\omega_i} > \sqrt{2} - \frac{M\cos\theta}{1 + \omega_d/\omega_i}, \tag{2}$$

where $M \equiv u/c_s$ is the Mach number and θ is the angle between $\mathbf{k}$ and $\mathbf{u}$. Note that modes with $\cos\theta > \sqrt{2}/M$ are stable even in the collisionless limit.

Consider a typical experiment [5] in krypton gas, with

$$a = 3.5\ \mu\text{m}, \qquad m_d = 2.7 \times 10^{-10}\ \text{g},$$
$$n_d \approx 3.6 \times 10^4\ \text{cm}^{-3} \quad \text{(within the dust cloud)}. \tag{3a}$$

For our "typical" case, we also assume

$$T_e = 3\ \text{eV}, \qquad n_e = n_i = 2 \times 10^9/\text{cm}^3,$$
$$T_e/T_i = 24, \qquad \text{and } M = 1 \quad \text{or} \quad M = 0.5. \tag{3b}$$

However, it should be noted that none of the parameters in (3b) is actually measured in the experiment. (The parameters n_e, n_i, T_i, and u all vary rapidly in or near the sheath and are very difficult to measure at the actual location of the dust cloud.) For this case, at $M = 1$ marginal stability occurs at $P \approx 260$ mTorr. It may be noted that in the experiments [5] the dust is seen to be in a fluid phase at $P = 167$ mTorr, but in a crystalline phase at 220 mTorr. Thus, given the uncertainties in the experimental parameters, it is very plausible that the phase transition from dust gas to dust solid is associated with the stabilization of the two-stream instability. To study this further, we have performed particle simulations which are discussed in Secs. 3 and 4.

A very useful approximation can be made in the dispersion relation (1), which is quite accurate for the *collisional* two-stream instability (but less so for the more familiar collisionless case). Since $\omega \ll \mathbf{k}\cdot\mathbf{u}$ and $\omega \ll \nu_i$, the term ω may be omitted in the denominator of the last term. The dispersion relation then reduces to

$$0 = 1 + \frac{1}{k^2\lambda_{\text{De}}^2} - \frac{\omega_d^2}{\omega(\omega + i\nu_d)} - \frac{\omega_i^2}{\mathbf{k}\cdot\mathbf{u}(\mathbf{k}\cdot\mathbf{u} - i\nu_i)}, \tag{4}$$

which is quadratic in ω, so that a complete stability analysis is easily done in closed form. Equation (4) reproduces the stability boundary (2) exactly, and the spectrum $\omega(k)$ to an accuracy of better than 1% for typical dusty plasma parameters.

3. The DSD simulation code.—Simulation of dusty plasma is difficult because the mass of a dust grain is $\sim 10^{12}$ times larger than that of an ion, so the time scales for grain motion are enormously slower than those for ions or electrons. To resolve this problem in a numerically efficient way, we have developed the "DSD" (dynamically shielded dust) code [10], in which only dust grains are represented as simulation particles. Electrons and ions do not appear as particles. However, the interaction between grains is the *dynamically shielded* Coulomb interaction [11,12], i.e., the Coulomb interaction mediated by the *complete* linear response of the plasma ions [distribution function $f_{i0}(\mathbf{v})$, streaming Maxwellian at temperature T_i and streaming velocity $\mathbf{u}$] and the warm electrons, including wakefields, ion-neutral collisions, and Landau damping. In k space the potential of one grain is given by

$$\phi(\mathbf{k}) = \frac{Ze/2\pi^2k^2}{1 + \dfrac{1}{k^2\lambda_{\text{De}}^2} + \dfrac{\omega_{pi}^2}{k^2}\dfrac{\int d^3\mathbf{v}\,\dfrac{\mathbf{k}\cdot\partial f_{i0}(\mathbf{v})/d\mathbf{v}}{\omega - \mathbf{k}\cdot\mathbf{v} + i\nu_i}}{1 - i\nu_i\int d^3\mathbf{v}\,\dfrac{f_{i0}(\mathbf{v})}{\omega - \mathbf{k}\cdot\mathbf{v} + i\nu_i}}} \tag{5}$$

and (since the plasma is treated by linear theory) the total potential is assumed to be given by the superposition of grain potentials. Pictures of the potential (5) in real space are shown in the first paper in Ref. [10]. To resolve both the long- and short-range forces, DSD uses the particle-particle/particle mesh technique of Hockney and Eastwood [13].

Since the DSD model includes only the dust grains as simulation particles, it may be a surprise that the two-stream instability is present in the code. However, the dielectric representation of the ions and electrons contains all the information needed, and the dispersion relation (4) may indeed be derived from the DSD model. [The model leads to the dispersion relation (4) rather than (1), because the grains are regarded as stationary in calculating the dielectric, a very good approximation which has also been used by all previous workers to calculate wakefields for dusty plasma.]

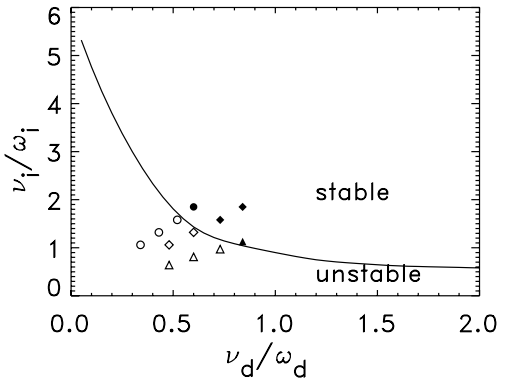

FIG. 1. The curve is the stability boundary in the $\nu_d/\omega_d - \nu_i/\omega_i$ plane. Each point corresponds to the parameters for a single DSD simulation. Triangles: homogeneous dust fill, $M = 0.5$. Diamonds: homogeneous dust fill, $M = 1$. Circles: confined dust cloud, six layers thick, $M = 1$. Open symbols indicate unstable cases; filled symbols indicate stable cases.

To study the nonlinear effect of the instability on the dust, we first performed a series of simulations where the dust grains form a uniform fluid filling the simulation box. Since the simulation is periodic, this corresponds to an infinite uniform medium and should reproduce the characteristics of the dispersion relation (4) exactly. The parameters were given by (3), at pressures 150, 200, 250, 300, and 350 mTorr, and at Mach numbers $M = 0.5$ and $M = 1$. Stable cases could easily be distinguished from unstable cases: In unstable cases, electrostatic modes grew exponentially through several orders of magnitude and eventually saturated; for stable cases, the electrostatic energy was thermal. In terms of ν_d/ω_d and ν_i/ω_i, the transition from stability to instability occurred exactly at the stability boundary predicted by theory, as shown in Fig. 1. The predicted critical pressure for stability $P_{\rm crit}$ is 330 mTorr at $M = 0.5$ and is 260 mTorr for $M = 1$. ($P_{\rm crit}$ decreases as M increases because ν_i is an increasing function of the ion velocity u.) The mode structure is generally in accordance with the dispersion relation (4) [14]. For example, the most unstable modes propagate along the streaming direction $\mathbf{u}$ for cases with $M = 0.5$, but obliquely to $\mathbf{u}$ for $M = 1$. In Fig. 2, we show the value of T_d after steady state has been reached for each of the simulations. Note the sharp increase in T_d for $P < P_{\rm crit}$.

4. Dust cloud simulations.—In discharge experiments, the dust accumulates in a disk-shaped region near the sheath edge at the lower electrode, where there is a vertical balance between gravity and the sheath electric field. The grains are typically confined laterally by electric fields resulting from the electrode geometry. To simulate this in DSD, we impose a vertical electric field which increases linearly with z, and a much weaker radial confining field which increases linearly with r. We initiate the grains at random positions in the simulation box. The grains rapidly collapse toward the equilibrium region, acquiring a large kinetic energy in the process, and this kinetic energy is equilibrated by grain-grain collisions. Thus, at an early time, the grains form a weakly coupled disk-shaped cloud. At high pressure, the grains then lose energy due to friction on the neutral gas, eventually become strongly coupled, and settle into a stationary configuration which is highly ordered. An example is shown in Figs. 3a and 3b for 1000 grains in a krypton discharge at pressure 350 mTorr, plasma parameters (3), and ions streaming at $M = 1$. Figure 3a shows the projection of the grains onto the x-z plane. Note that the grains are stratified into six layers. Figure 3b shows the projection onto the x-y (transverse) plane and shows mostly hexagonal short-range order, and even a substantial degree of long-range order. To give some indication of the vertical structuring, in Fig. 3b grains that are located in the top region, $z > 15.1\lambda_{\rm De}$, are shown as blue diamonds, and grains in the bottom region $z < 15.9\lambda_{\rm De}$ are shown as red circles. Note that nearly every blue diamond overlaps a red circle, indicating that the grains are arranged into vertical columns. Other structural features can be discerned and are discussed elsewhere [10]. The ordering is very similar to what is seen in dust crystallization experiments [1–6].

For pressure below $P_{\rm crit} = 330$ mTorr, the simulation shows a very different picture. The grains collapse into

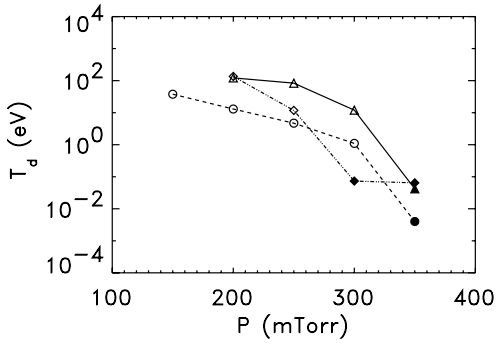

FIG. 2. T_d as a function of P. Triangles: homogeneous dust fill, $M = 0.5$. Diamonds: homogeneous dust fill, $M = 1$. Circles: confined dust cloud, six layers thick, $M = 1$. Open symbols indicate unstable cases; filled symbols indicate stable cases.

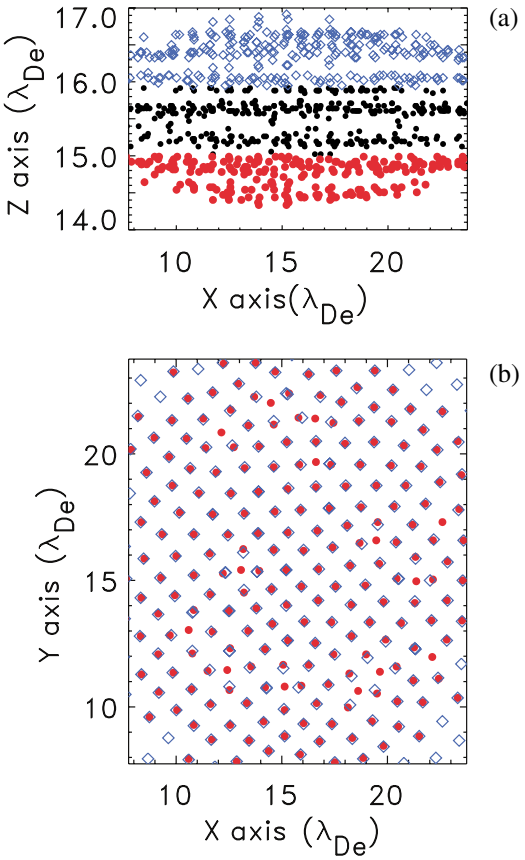

FIG. 3 (color). Snapshot of grain locations, for a simulation with $P = 350$ mTorr (stable). (a) Projection of the grains onto the x-z plane. (b) Projection of the grains onto the x-y plane. The streaming direction is z. Blue diamonds indicate grains located in the top region $15.9\lambda_{\rm De} < z$, black dots indicate grains in the middle region $15.1\lambda_{\rm De} < z < 15.9\lambda_{\rm De}$, and red circles indicate grains in the lower region $z < 15.1\lambda_{\rm De}$.

a dust cloud which remains hot, fluidlike, and nearly unstructured. For $P = 150$ mTorr, e.g., T_d reaches a final steady-state value ≥ 25 eV (which is 8 times T_e, and orders of magnitude larger than the ion or neutral temperature), despite the continuing frictional dissipation of grain kinetic energy, and the absence of any explicit mechanism in the code that heats the grains. The heating of the grains can be due only to the two-stream instability.

In Fig. 2, we have also plotted T_d against P for five dust cloud simulations (shown as circles) at pressures 150 to 350 mTorr, including the two cases discussed above. In all cases, the plasma parameters are given by (3) and $M = 1$. Note the sudden increase in T_d when P falls below $P_{\text{crit}} = 330$ mTorr. The parameters for the five simulations are also plotted as circles in the dimensionless space $\nu_i/\omega_i - \nu_d/\omega_d$ in Fig. 1. The critical pressure for the dust cloud is greater than P_{crit} for the homogeneous simulation. Because of the confining forces, the cloud grain density is approximately twice as large as the homogeneous grain density. The resulting higher plasma frequency ω_d requires a larger ν_d and thus a higher pressure for stabilization. Even for the dust cloud, stabilization occurs at the point predicted by the dispersion relation (4), so neither the inhomogeneity of the dust cloud nor the presence of confining forces seems to affect the stability condition. However, the collisional two-stream instability is convective in the dust frame [14], so the instability growth is limited by the thickness of the cloud. As a result, T_d is smaller for a bounded cloud than for unbounded homogeneous dust, as seen in Fig. 2.

5. Discussion.—We conclude that two-stream instability is the explanation for the high kinetic temperature of the dust grains in low-pressure experiments, and the collisional stabilization of the two-stream instability is the trigger for condensation of the dust into a solid state. Instability calculations show good quantitative agreement with dust cloud simulations, and qualitative agreement with experiments, even though the theory strictly applies only to an infinite homogeneous medium. The details of the mechanism by which the instability heats grains, and the detailed kinetics of the dust phase transition, are being studied and will be discussed in future papers.

Schweigert *et al.* [6] have explained the melting of the crystalline state in terms of phonons driven unstable by the presence of wakes. There is no reason to expect that the level of collisionality necessary to stabilize the phonon instability is the same as the collisionality necessary to stabilize the two-stream instability for fluid-phase dust. If the critical pressure for melting a dust crystal is higher than P_{crit} for freezing a dust fluid, it follows that there is a range of pressures where both the solid and fluid phases of the dust are stable, and one may expect a mixed-phase system, as has been observed [5]. Although the dust grains emphatically do not constitute a closed system, this is analogous to first-order phase transition phenomena in a thermodynamic system.

This work was supported by NASA and ONR. The authors are grateful to K. (Dennis) Papadopoulos for useful suggestions regarding the linear dispersion relation.

*Email address: joyce@nrl.navy.mil

[1] A. Melzer, A. Homann, and A. Piel, Phys. Rev. E **53**, 2757 (1996).
[2] H. Thomas *et al.,* Phys. Rev. Lett. **73**, 652 (1994).
[3] J. H. Chu and Lin I, Phys. Rev. Lett. **72**, 4009 (1994).
[4] A. Melzer, T. Trottenberg, and A. Piel, Phys. Lett. A **191**, 301 (1994).
[5] H. Thomas and G. E. Morfill, Nature (London) **379**, 806 (1996); J. Vac. Sci. Technol. A **14**, 501 (1996).
[6] V. A. Schweigert *et al.,* Phys. Rev. E **54**, 4155 (1996); Phys. Rev. Lett. **80**, 5345 (1998).
[7] F. Melandso, Phys. Rev. E **55**, 7495 (1997).
[8] R. A. Quinn and J. Goree, Phys. Rev. E **61**, 3033 (2000); Phys. Plasmas **7**, 3904 (2000).
[9] O. Havnes, Astron. Astrophys. **193**, 309 (1988); R. Bharuthram, H. Saleem, and P. K. Shukla, Phys. Scr. **45**, 512 (1992); D. Winske *et al.,* Geophys. Res. Lett. **22**, 2069 (1995); M. Rosenberg, J. Vac. Sci. Technol. A **14**, 631 (1996); D. Winske and M. Rosenberg, IEEE Trans. Plasma Sci. **26**, 92 (1998).
[10] M. Lampe, G. Joyce, and G. Ganguli, Phys. Plasmas **7**, 3851 (2000); IEEE Trans. Plasma Sci. **29**, 238 (2001); Phys. Scr. **T89**, 106 (2001).
[11] N. Rostoker and M. N. Rosenbluth, Phys. Fluids **3**, 1 (1960).
[12] N. A. Krall and A. W. Trivelpiece, *Principles of Plasma Physics* (McGraw-Hill, New York, 1973), Chap. 11.
[13] R. W. Hockney and J. W. Eastwood, *Computer Simulation Using Particles* (Adam Hilger, Bristol, 1988), Chaps. 8 and 12.
[14] More details on these points will be given in a subsequent publication.